It is possible to estimate ΔH^*(M–CO) from the measured bond enthalpies, ΔH°,[25] estimated valence reorganization enthalpies, $\Delta H_{CO^\bullet}{}^{M}$,[27] and the approximation $\Delta H_{M^\bullet}(Mo) \approx \Delta h_{M^\bullet}(W) \approx 80$ jK/mol (i.e. $^1/_2\Delta H_{M^\bullet}(Cr)$). These values for the "intrinsic" bond enthalpies (ΔH^*[E] in Table II) exhibit the order Mo < Cr ≈ W. Thus, the thermochemical bond enthalpy data are consistent with trends in bond enthalpies from spectroscopic and kinetic measurements *if*, as calculated by Ziegler et al.,[2] the valence promotion energy for Cr is substantially greater than for the 4d and 5d metals.

Conclusions

It has been suggested, on the basis of experimental IP's and charge-transfer spectra, that the π bond order increases monotonically within the group 6 metal hexacarbonyls.[29] However, we have observed here that the CO 2π-orbital populations calculated from $\chi(^{17}O)$ vary in the order $Mo(CO)_6 < Cr(CO)_6 \approx W(CO)_6$. This is the same order found for the majority (although not totality) of experimental quantities dependent upon the net, $\sigma + \pi$, M–CO bond strengths. From this comparison, one may conclude that variations in π bonding play an important role in determining relative bond strengths in group 6 hexacarbonyls. We note that this lends a degree of support for the results of recent theoretical investigations[2] which suggest that the total stability of the M–CO bond in transition-metal complexes is dominated by the π component.

Acknowledgment. We wish to thank Profs. Paul S. Braterman and Michael G. Richmond for helpful comments concerning the manuscript and the Robert A. Welch Foundation (Grant B-657) and UNT Faculty Research Fund for support of this research.

Contribution from the Department of Chemistry, University of Florida, Gainesville, Florida 32611

Molecular Orbital Investigation of Ruthenium–Oxo-Catalyzed Epoxidations

Thomas R. Cundari and R. S. Drago*

Received February 1, 1989

INDO/1 calculations were carried out with the aim of studying the various intermediates and pathways proposed for epoxidations involving high-valent, metal–oxo catalysts: *N*-oxo, oxometallacycle, open, bound epoxide, and caged radical intermediates. The model complex chosen was a six-coordinate Ru(IV)–oxo complex. The conversion of the Ru–oxo complex to a five-coordinate *N*-oxo intermediate was discounted due to the large energy barrier to migration of O to the nitrogen atom of a ligand. The formation of the oxometallacycle by a either a concerted or nonconcerted pseudo-[2 + 2] cycloaddition of C=C to Ru—O was found to be unfavorable. A concerted [1 + 2] addition was also found to be unfavorable. The calculations show that the unfavorable nature of these pathways is similar in origin to that of their better known organic analogues. The preferred pathway is a nonconcerted [1 + 2] cycloaddition to yield a bound epoxide. The reaction amounts to nucleophilic attack on the oxo oxygen. Since one C–O bond is formed first, and then the second, there is a buildup of radical cation behavior on the carbon that is not bound. Simple electrostatic considerations lead one to predict, and INDO/1 calculations agree, that attack of the unbound carbon on the electron-rich oxo (to yield bound epoxide by a nonconcerted [1 + 2] pathway) in preference to the high-valent Ru atom (to yield oxometallacycle by a nonconcerted [2 + 2] pathway). The results of the theoretical analysis are combined with experimental data in an attempt to clarify the important interactions that characterize this important reaction.

Introduction

Epoxidation is a commercially important process. In the year 1987, 5.62 billion pounds of ethylene oxide and 2.61 billion pounds of propylene oxide were produced in the United States.[1] The mechanisms by which the enzyme cytochrome P-450 and its inorganic porphyrin analogues oxidize various organic species has been an area of much focus.[2] Epoxidation of olefins, in particular, has gathered much attention.[3] The discovery by Groves and co-workers that Fe^{III}(TPP)Cl/PhIO (TPP = tetraphenylporphyrin) can perform chemistry similar to that of the cytochrome P-450/molecular oxygen system has fostered much research into the proposed Fe–oxo reactive intermediate.[4] Other workers have concentrated on different metals[5] and different oxygen atom transfer reagents.[6]

For epoxidations involving these metal–oxo complexes, many pathways and intermediates arising from the oxygen atom transfer step have been discussed. The [2 + 2] cycloaddition of the olefins to the metal–oxo bond to yield a four-membered ring structure, referred to alternatively as an oxometallacycle or metallaoxetane,[7] has been proposed. The work of Bruice[8] with *N*-oxo transfer reagents has led to the consideration of a process where a precursor with increased N (from a ligand)–O bonding is the active species. Direct oxygen atom transfer has been advanced to explain the stereospecificity of some systems,[9] while open intermediates have been invoked to explain stereochemical inversion in others.[10] Outer-sphere electron transfer,[11] to form a caged radical cation species, and a suicide complex[12] —a cyclic, five-membered, M–O–C–C–N intermediate—have also been forwarded.

Ruthenium–oxo catalysts have recently been reported that utilize molecular oxygen to epoxidize norbornadiene and styrene.[13,14] We have carried out semiempirical molecular orbital calculations on a Ru(IV)–oxo complex with the intent of studying the various pathways and intermediates that have been postu-

(1) Reisch, M. C. *Chem. Eng. News* **1988**, *66* (15), 30.
(2) (a) Groves, J. T. *J. Chem. Educ.* **1985**, *62*, 1928. (b) *Cytochrome P-450*; Ortiz de Montellano, P. R. Ed.; Plenum: New York, 1986.
(3) (a) Castellino, A. J.; Bruice, T. C. *J. Am. Chem. Soc.* **1988**, *110*, 158. (b) Castellino, A. J.; Bruice, T. C. *J. Am. Chem. Soc.* **1988**, *110*, 7512. (c) Garrison, J. M.; Bruice, T. C. *J. Am. Chem. Soc.* **1989**, *111*, 191.
(4) Groves, J. T.; Nemo, T. E.; Myers, R. S. *J. Am. Chem. Soc.* **1979**, *101*, 1032.
(5) (a) Ru: Dobson, J. C.; Seon, S. K.; Meyer, T. J. *Inorg. Chem.* **1986**, *25*, 1513. (b) Other transition metals: Holm, R. H. *Chem. Rev.* **1987**, *87*, 1401.
(6) Meunier, B. *Bull. Soc. Chim. Fr.* **1986**, 578.
(7) (a) Sharpless, K. B.; Teranishi, A. Y.; Backvall, J. E. *J. Am. Chem. Soc.* **1977**, *99*, 3120. (b) Rappé, A. K.; Goddard, W. A. *J. Am. Chem. Soc.* **1982**, *104*, 448. (c) Groves, J. T.; Nemo, T. E. *J. Am. Chem. Soc.* **1983**, *105*, 5786.
(8) Shannon, P.; Bruice, T. C. *J. Am. Chem. Soc.* **1981**, *103*, 4580.
(9) Groves, J. T.; Nemo, T. E. *J. Am. Chem. Soc.* **1983**, *105*, 5786.
(10) Sheldon, R. A.; Kochi, J. K. *Metal Catalyzed Oxidations of Organic Compounds*; Academic: New York, 1981; p 176.
(11) Traylor, T. G.; Nakano, T.; Dunlap, B. E.; Traylor, P. S.; Dolphin, D. *J. Am. Chem. Soc.* **1986**, *108*, 2782.
(12) Collman, J. P.; Hampton, P. D.; Brauman, J. I. *J. Am. Chem. Soc.* **1986**, *108*, 7861.
(13) Groves, J. T.; Quinn, R. *J. Am. Chem. Soc.* **1985**, *107*, 5790.
(14) Bailey, C. L.; Drago, R. S. *J. Chem. Soc., Chem. Commun.* **1987**, 179.

0020-1669/90/1329-0487$02.50/0

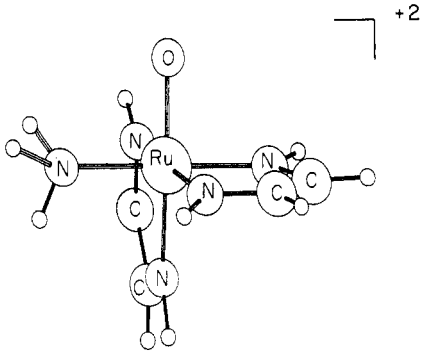

Figure 1. Structure of the ruthenium–oxo model compound containing two glyoxal diimines and a ammonia ligand. The *xy* plane is perpendicular to the Ru–oxo bond.

lated[7-12] for transition-metal-catalyzed oxygen atom transfer reactions involving high-valent, metal–oxo complexes. The Ru–oxo system was chosen as it is a well-characterized epoxidation system that is similar to the iron-based biological systems.

It is the aim of the present paper to use INDO/1 calculations to understand the metal–oxo/olefin reaction from a point of view of simple frontier orbital considerations and to combine theoretical and experimental evidence to yield a coherent picture of this important reaction. The shortcomings of SCF methods (semiempirical[15] as well as ab initio[16]) in describing *quantitatively* the electronic structure of transition-metal complexes are well-known. These limitations should be kept in mind. Conclusions must be drawn within the framework of basic electronic structural arguments. The semiempirical INDO/1 model was chosen due to the large size of the reacting system, the presence of polar bonds, and the fact that the method has been shown to describe the ground and low-energy excited states for similar systems very well.[17-19]

Calculations

The theoretical method used here was the semiempirical INDO/1 formalism.[15,20] Various modes of ethylene addition to our model compound, *cis*-$[Ru(HN{=}CH{-}HC{=}NH)_2(NH_3)(O)]^{2+}$ (Figure 1) were studied to probe reaction intermediates that have been proposed. To reduce the overall basis set size, glyoxal diimine was used in the calculation to model the phenanthroline, pyridyl, and porphyrin ligands actually used in experimental work; bipyridine parameters (bond lengths and angles) were used for glyoxal diimine[21] and free ammonia values[21] for the ammonia ligand. Gradient-driven geometry optimizations of olefin and $RuOL_5^{2+}$ moieties were carried out for each Ru–oxo/ethylene separation/orientation to yield stationary points on the potential energy surface. Convergence to a stationary point on the potential energy surface was assumed when the gradient was less than 5.0×10^{-3} hartree/bohr. In all cases, energies converged well within 1 kcal mol^{-1}. Furthermore, selection of a lower gradient convergence threshold did not affect the results significantly despite the increase in computational time and cost. The initial orientation of the ethylene versus the Ru–oxo moiety is significant in that it defines the various interatomic interactions. At relatively close distances ($R_{CO} < 2.7$ Å), the energy of interaction between the ethylene and the transition-metal complex, in all coordination modes directed at the oxo moiety, was calculated to decrease monotonically and led to covalently bound stationary points. Therefore, our conclusions are pertinent to the reaction pathway after the reactants have passed the small activation energy barrier, $R_{CO} \approx 2.7$ Å.

Table I. Calculated Orbital Energies for RuO

MO[b]	spin	ON[c]	energy[a] ab initio	energy[a] INDO/1
RuO π	β	2	−0.431	−0.431
RuO π	α	2	−0.594	−0.622
Ru σ	α	1	−0.561	−0.527
RuO π^* *d*	α	2	−0.398	−0.409
Ru δ[d]	α	1	−0.631	−0.543
Ru 5s[d]	α	1	−0.292	−0.309
RuO π^*	β	0	0.066	0.064

[a] The energies of the spin orbitals of RuO ($^5\Delta$) are given in au. [b] An orbital designated RuO is delocalized over both the Ru and O atoms; those designated Ru are localized to the greatest extent on the metal. [c] ON is the occupation number for the given spin orbital. An occupation number of 2 signifies two singly occupied spin orbitals in a degenerate pair. [d] These orbitals are unparied; i.e., their β counterpart is unoccupied.

Table II. Calculated Observables for RuO^+ [a]

MO	spin	ON	energy ab initio	energy INDO/1
RuO π	β	2	−0.590	−0.669
RuO π	α	2	−0.896	−0.852
Ru δ[b]	α	1	−0.781	−0.796
RuO π^* [b]	α	2	−0.714	−0.678
RuO π^*	β	0	−0.200	−0.205

[a] The energies of the spin orbitals of RuO^+ ($^4\Delta$) are given in au. For other specifics see the footnotes in Table I. [b] These orbitals are unpaired, i.e. their β counterpart is unoccupied.

The atomic bond index used in the MO analysis (vide infra) is defined as

$$B_{AB} = \sum_{u}^{\text{on A}} \sum_{v}^{\text{on B}} P_{uv}P_{vu} \tag{1}$$

where the summation is over all atomic orbitals $|\chi_u\rangle$ and $|\chi_v\rangle$ on atoms A and B, respectively and P_{uv} is the bond order or density matrix element between $|\chi_u\rangle$ and $|\chi_v\rangle$. The atomic bond index yields a value of 1 for a single bond, 2 for a double bond, etc. P_{uv} is defined as

$$P_{uv} = \sum_{i}^{\text{occ}} c_{ui}c_{vi} \tag{2}$$

where c_{ui} and c_{vi} are the AO coefficients of $|\chi_u\rangle$ and $|\chi_v\rangle$ in MO $|\Psi_i\rangle$ using the LCAO–MO approximation.

A series of test calculations, using the INDO/1 model as derived by Zerner and co-workers[15,20b,22b] for transition-metal species, was carried out on various second-row transition-metal compounds (Y to Ag) to ascertain the suitability of the INDO/1 method for the present study. The results show that the INDO/1 model yields quality results with respect to quantities such as equilibrium geometries, orbital energies, atomic charges, energy ordering of geometric isomers, etc.

Although it is not the purpose of the present paper to engage in an analysis of the INDO/1 model as pertains to second-row transition-metal compounds, some discussion of pertinent results is warranted. Some equilibrium geometry results are given in eq 3 (Cp = η^5-C_5H_5; N =

RuO^+ ($^4\Delta$) (r_e = 1.75 Å (ab initio/CI[23a]), 1.72 Å (INDO)) (3a)

RuO ($^5\Delta$) (r_e = 1.75 Å (ab initio/CI[23b]), 1.74 Å (INDO)) (3b)

RuO_4 (r_e = 1.705 Å (expt[23c]), 1.704 Å (INDO)) (3c)

$Ru^{IV}N_5O^{2+}$ (r_e(Ru–O) = 1.77–1.86 Å (expt[24]), 1.96 Å (INDO)) (3d)

$Ru^{VI}N_4(O)_2^{2+}$ (r_e(Ru–O) = 1.71–1.72 Å (expt[24]), 1.71 Å (INDO)) (3e)

$RuCp_2$ (r_e(Ru–C) = 2.20 Å (expt[23d]), 2.15 Å (ab initio[23d]), 2.24 Å (INDO)) (3f)

(15) A discussion of these problems and the steps taken to circumvent them are given in: Bacon, A. D.; Zerner, M. C. *Theor. Chim. Acta* **1979**, *53*, 21.
(16) Some of these problems are discussed in: *Quantum Chemistry: The Challenge of Transition Metals and Coordination Chemistry*; Veillard, A., Ed.; Reidel: Dordrecht, The Netherlands, 1986; p 235.
(17) Loew, G. H.; Kert, C. J.; Hjelmeland, L. M.; Kirchner, R. F. *J. Am. Chem. Soc.* **1979**, *99*, 3534.
(18) Loew, G. H.; Herman, Z. S. *J. Am. Chem. Soc.* **1980**, *102*, 6173.
(19) Hanson, L. K.; Chang, C. K.; Davis, M. S.; Fajer, J. *J. Am. Chem. Soc.* **1981**, *103*, 663.
(20) (a) Pople, J. A.; Beveridge, D. L. *Approximate Molecular Orbital Theory*; McGraw-Hill: New York, 1970. (b) Anderson, W.; Edwards, W. D.; Zerner, M. C. *Inorg. Chem.* **1986**, *25*, 2728.
(21) *Interatomic Distances*; Sutton, L. E., Ed.; The Chemical Society: London, 1958.
(22) (a) The results for the geometry optimizations and the use of the INDO/1 method for the calculation of other properties is discussed in further detail for various ruthenium species in: Cundari, T. R.; Drago, R. S. *Int. J. Quantum Chem.*, in press. (b) Results for the second-row transition metals from Y to Ag (including Ru) are presented in: Cundari, T. R.; Anderson, W.; Zerner, M. C.; Drago, R. S. *Inorg. Chem.*, in press.

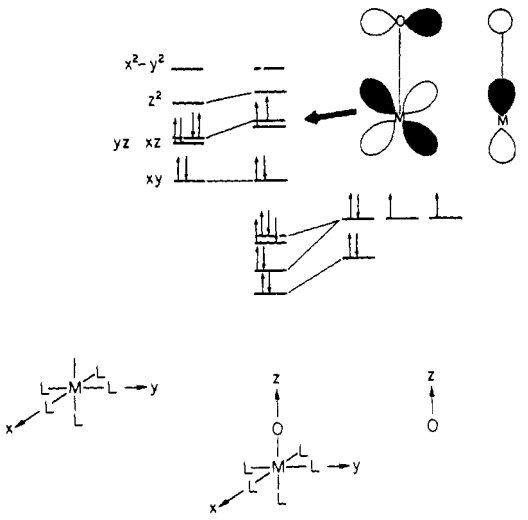

Figure 2. MO interaction diagram for a C_{4v}, d^6 RuL_5^{2+} fragment and an oxygen atom (^3P). The important e_x^* and e_y^* MO's are shown. L is assumed to be predominantly a σ donor.

neutral nitrogen ligand, e.g. bpy or phen for expt and glyoxal diimine or NH_3 for INDO). These results agree well with experiment (where available) and high-level ab initio calculations (some of which include CI).

Calculations of orbital energies for RuO and RuO^+ are shown in Tables I and II, respectively. The methods used for the ab initio routine have been given elsewhere.[22a]

The INDO/1 method performs well in the calculation of energy differences of isomers. In the absence of experimental evidence, the agreement must be labeled qualitative. It is too much to ask any SCF-based method (i.e. where electron correlation is neglected) to *quantitatively* predict absolute thermodynamic data. However, as the integrals and parameters that characterize semiempirical methods are derived from experiment, electron correlation is included in some way. Any MO method must be capable, however, of at least yielding qualitative agreement with experiment. For example, simple theoretical concerns predict (and experiment supports) that d^0 four- and five-coordinate complexes (e.g. $ZrCl_4$ and $NbCl_5$, respectively) should possess tetrahedral and trigonal-bipyramidal coordination geometries, respectively. Similarly, d^8 four-coordinate complexes (e.g. $PdCl_4^{2-}$) will be square planar. The INDO/1 model faithfully predicts these equilibrium geometries as well as others. Given the paucity of experimental information about M–C and M–O bond strengths, we must rely on qualitative arguments to critically evaluate the INDO results.

Results and Discussion

1. Electronic Structure of the Transition-Metal–Oxo Fragment. The qualitative MO interaction diagram for a d^6, C_{4v}, $Ru^{II}L_5^{2+}$ fragment interacting with an oxygen atom (^3P ground state) is given in Figure 2. The RuO π system, as noted in this present research and by other workers for the ruthenium–oxo systems, has a significant covalent contribution.[22,23a,b] The ruthenium–oxo species is similar to O_2 in that both have low-energy singlet and triplet states,[24] and a $\sigma^2\pi^4\pi^{*2}$ electronic configuration. A geometry optimization of the model compound, Figure 1, results in a pseudooctahedral compound with a Ru–O bond length of 1.96 Å, Ru–N bond lengths of ≈2.06 Å, and all L–M–L angles of ≈90°. The Ru–N bond lengths are in good agreement with the experimental values of Ru–N = 2.07–2.16 Å[25] and Ru–O = 1.75–1.86 Å[25] for Ru(IV)–oxo complexes with nitrogen ligands.

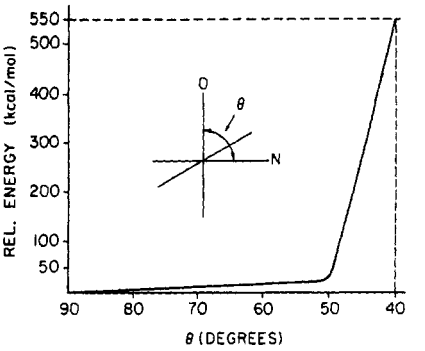

Figure 3. Total energy as a function of θ, the angle between O, Ru, and an equatorial N atom from a ligand.

2. Reaction Pathways. Three basic reaction pathways were considered for epoxidation: formation of an *N*-oxo intermediate, concerted metal–oxo/olefin interaction, and olefin attack on the oxo functionality.

a. Formation of an *N*-Oxo Intermediate. The transformation of the metal–oxo species to an *N*-oxo species has been proposed for the iron–oxo–porphyrin system.[26a] A potential energy surface, triplet spin state, was constructed for the distortion mode that converts the Ru–oxo complex to a species with increased N–O bonding. The N_{eq}–Ru–O angle, θ, was compressed from 90°, to allow comparison with the results of Veillard[26b] and Jorgensen.[26a] A soft potential energy surface resulted up to θ = 50°, after which the total energy, Figure 3, increases markedly. Up to θ = 50° there is no N–O bonding, as evidenced by a maximum atomic bond index of 0.06 and a minimum N–O distance of 1.67 Å on the shallow portion of the potential energy surface. Stabilization of the HOMO (π^*) of the Ru–oxo system, due to a decrease in the unfavorable overlap of the $d\pi$–$p\pi$ antibonding combination, is counteracted by a destabilization of the $d\pi$–$p\pi$ bonding combination (caused by a decrease in the favorable π overlap). The doubly occupied bonding combination dominates the singly occupied antibonding combination with respect to their effects on the overall energetics. These considerations lead to a high energy barrier for *N*-oxide formation and reduce the possibility of the *N*-oxo mechanism for ruthenium. The results for $Ru^{IV}L_5O^{2+}$ are in agreement with the ab initio analysis of Strich and Veillard[26b] on $Fe^{IV}OP$–py (P = porphyrin dianion, py = axial pyridine), who found an *N*-oxo intermediate to be unfavorable but opposite to the extended Hückel results of Jørgensen[26a] on $Fe^{IV}OP$–OH_2.

b. Concerted [2 + 2] Metal–Oxo/Olefin Interaction. Next, the concerted formation of an oxometallacycle was studied. This amounts to a pseudo-[2 + 2] cycloaddition. This pathway is analogous to the least-motion, D_{2h} pathway for the formation of cyclobutane from two ethylenes—a forbidden process. Geometry optimization of structures where the Ru–O and C–C σ bonds are parallel, the C–C σ bond is perpendicular to the *xy* plane of the complex, and the Ru–C distance is slightly larger than a typical covalent Ru–C bond ($R_{RuC} \approx 2.43$ Å, compared with $R_{RuC} \approx 2.12$ Å for ruthenocene[21]) resulted in energy-minimized intermediates with almost no bonding between the ethylene and transition-metal–oxo fragments. The C–C bond length was little changed from the 1.332 Å of free ethylene,[21] the hydrogen atoms on the ethylene did not bend back toward tetrahedral angles, the Ru–O bond did not lengthen significantly, and the equatorial ligands did not bend away to accommodate ethylene coordination. This calculation was repeated with the pentammine analogue of our model compound instead of the chelating ligands (in our simulation glyoxal diimine), which are normally used. The pentammine model possesses more freedom in its bending modes and is more likely to distort out of the way to accommodate an oxometallacycle. Results similar to those observed for the chelating ligands were observed. Optimization of a "forced" oxometallacycle, using the pentammine analogue, where the equatorial ligands were bent back

(23) (a) Goddard, W. A.; Carter, E. A. *J. Phys. Chem.* **1988**, *92*, 2874. (b) Krauss, M.; Stevens, W. J. *J. Chem. Phys.* **1985**, *82*, 5584. (c) Sneddon, E. A.; Sneddon, L. G. *The Chemistry of Ruthenium*; Clark, R. J. H., Ed.; Elsevier: Amsterdam; p 43. (d) Pietro, W. J.; Hehre, W. J. *J. Comp. Chem.* **1983**, *4*, 241.
(24) (a) Moyer, B. A.; Meyer, T. J. *Inorg. Chem.* **1981**, *20*, 436. (b) Meyer, T. J. Presented at the Symposium on Atom Transfer Reactions, 197th National Meeting of the American Chemical Society, Dallas, TX, April 1985; INOR 13. (c) Mayer, J. M.; Nugent, W. A. *Metal-Ligand Multiple Bonds*; Wiley: New York, 1988.
(25) Che, C.-M.; Lai, T.-F.; Wong, K.-Y. *Inorg. Chem.* **1987**, *26*, 2289.
(26) (a) Jørgensen, K. A. *J. Am. Chem. Soc.* **1987**, *109*, 698. (b) Strich, A.; Veillard, A. *Theor. Chim. Acta* **1981**, *60*, 379.

and covalent C–O and Ru–C bond distances were used (an approximately pentagonal bipyramidal structure) as a starting point, resulted in the Ru–oxo complex reverting to six-coordination and the ethylene dissociating from the metal complex upon minimization. These results suggest that concerted oxometallacycle formation by a [2 + 2] cycloaddition pathway is an unfavorable pathway.

The INDO/1 results are consistent with a process similar to that for the dimerization of ethylene. As the two π systems approach each other the interaction between the π-bonding MO's (Ru dπ–O pπ and C pπ–C pπ) is increased. These MO's interact as they are close in energy and have similar nodal patterns. As both are doubly occupied, the interaction is repulsive. It is this repulsive interaction that leads to the unfavorable nature of the concerted [2 + 2] pathway. Although quantitative description of the PES is not expected, any MO method will calculate a two-orbital, four-electron interaction to be repulsive.

c. Concerted [1 + 2] Ru–Oxo/Olefin Interaction. Initial Formation of an Ion–Molecule Complex. The [1 + 2] pathway is analogous to the least-motion pathway for the formation of cyclopropane from methylene and ethylene—a forbidden process. At separations greater than $R_{C-oxo} \approx 2.7$ Å, energy minimization leads to the formation of a weakly bound (by $\approx$9 kcal mol^{-1}) ion ($RuL_5O^{+2-\delta}$)–molecule ($C_2H_4^{+\delta}$) complex. This ion–molecule complex is interesting in that it is similar to the charge-transfer complex that has been proposed by Bruice in the epoxidation of olefins by oxo–chromium porphyrins.[27] The ground state for this complex is a triplet. Covalent C–oxo bonding is virtually nonexistent (atomic bond index $\approx$ 0.0), and the Ru–oxo/olefin interaction is largely electrostatic. This intermediate differs significantly from the caged radical cation proposed by various workers[11] in that less than a full electron ($\approx$0.1 electron) is transferred. The carbon–carbon π-bonding is essentially intact (atomic bond index = 1.86) in this intermediate so that rotation about the C–C bond does not occur in the ion–molecule complex.

Proceeding along the [1 + 2] pathway from the shallow ion–molecule minimum toward covalently bound species, i.e. bound epoxides, incurs a small barrier, <3 kcal mol^{-1}, at $R_{C-oxo} \approx 2.5$ Å. Geometry optimization after this barrier has been passed leads to local minima that indicate bound epoxides—but not by a concerted pathway. These bound epoxides possess a singlet ground state, not at all surprising since they are d^6 pseudooctahedral complexes. The preference for the [1 + 2] pathway and intermediate will be discussed later. The unfavorability of the concerted pathway arises from the repulsive four-electron, two-orbital interaction between the oxo lone pair (largely O 2p$_z$) and the olefin π MO.

d. MO Analysis of the Oxo/Olefin Reaction Pathway. Four distinct trajectories were considered for attack of the ethylene on the oxo atom in order to characterize the nonconcerted pathways: on-center–perpendicular; on-center–canted; off-center–perpendicular; off-center–canted. On-center and off-center refer to orientations in which the center of the C-C bond is colinear and noncolinear with the Ru and O atoms, respectively. Perpendicular and canted refer to orientations of the molecular plane of ethylene perpendicular and canted (by 30°), respectively, relative to the vector that describes the metal–oxo bond (Figure 4). In the process of canting, the rotation axis is the C–C σ bond, so that canting, by itself, keeps the C–oxo distances equal. These four pathways lead to bound epoxide intermediates with two distinct modes for coordinating the resulting ethylene oxide (vide infra). In all cases, the geometry optimization locked into local minima for the final bound epoxide.

As mentioned previously, these geometry optimizations lead to local minima that indicate bound epoxides. The Ru–oxo bond lengthens to 2.1 Å in the bound epoxides. These results are in line with the Ru–O bond lengths of 2.03 Å in *trans*-$Ru(NH_3)_4(NO)(OH)$[21] and 2.07 Å for *trans*-$RuCl_4(NO)(OH)$.[21] The bond lengths in the bound ethylene oxides are 1.50 Å for the C–C bond (1.47 Å in free ethylene oxide[21]) and 1.43 Å for the C–O bonds (1.44 Å in free ethylene oxide[21]). In all cases, the bound epoxide has equal C–O and C–H bond lengths with local C_{2v} symmetry for the epoxide moiety.

The electronic structure of the bound epoxide is of interest itself. The oxygen in ethylene oxide possesses the two lone pairs (**1a**; see Scheme I) of hybrid orbital theory that correspond to the symmetric (σ, **1b**) and antisymmetric (π, **1c**) nonbonding orbitals of MO theory. A coplanar RuOCC geometry allows the epoxide to act as both a σ and π donor. Bending the epoxide ligand out of the plane diminishes the repulsive two-orbital, four-electron Ru dπ–epoxide O pπ interaction for the octahedral, d^6 system and thus leads to a lower energy conformation.

3. Nonconcerted [2 + 2] Pathways Leading to Oxometallacycle Formation. It is necessary to investigate the possible formation of an oxometallacyclic intermediate after carbon–oxygen bond formation takes place, i.e. in a nonconcerted fashion. Nonconcerted pathways link the concerted [1 + 2] and [2 + 2] pathways. Both are characterized by the formation of one covalent C–O bond and possess an unbound terminal carbon. The major difference is the Ru–O–C angle. The nonconcerted [2 + 2] pathways have angles closer to 90°. The nonconcerted [1 + 2] pathways have angles closer to 180° and less steric repulsions between the olefin fragment and the ligands. The structures in Chart I, each possessing differing amounts of metal–terminal-carbon interaction, as determined by the interatomic distance, were subject to geometry optimizations. It must be stressed that the open structures in Chart I are not isolated, stationary points on the potential energy surface. The metal–carbon distance varied from 2.12 Å, the Ru–C distance in ruthenocene,[21] to over 3.5 Å. In all cases, even those with O to terminal C distances greater than the Ru–C distance, the direct formation of bound epoxide occurred. This preference

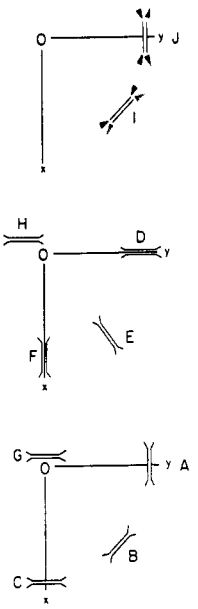

Figure 4. Various initial orientations of the ethylene fragment (viewed from the positive *z* axis) directed at the oxo moiety. I and J differ from A and B, respectively, in that the latter are parallel to the *xy* plane while the former are canted.

Scheme I. Schematic Diagram Showing the Relationship between the sp^3 Hybrids of VB Theory (**1a**) and the Nonbonding Orbitals of MO Theory (**1b** and **1c**)

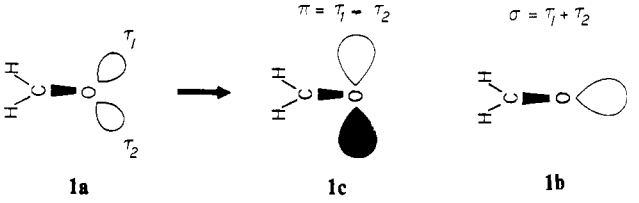

(27) Bruice, T. C. Presented at the Symposium on Atom Transfer Reactions, 197th National Meeting of the American Chemical Society, Dallas, TX, April 1985; INOR 48.

Chart I. Structures with One C–O Bond Broken That Were Submitted to Geometry Optimizations[a]

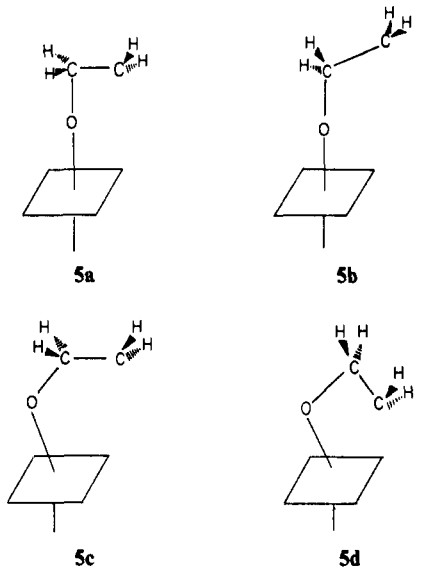

[a] Regardless of M–C distance, all led to bound epoxides rather than oxometallacycles.

Chart II. Starting Structure, before Energy Minimization, of the Forced Metallacycle (Bond Lengths in Å; Angles in deg)

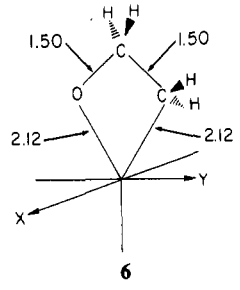

for bound epoxide over oxometallacycle is readily explained by electron density considerations. The loss of electron density on the terminal carbon causes it to interact preferentially with the higher electron density on the oxo, to form a bound epoxide, in preference to interaction with the lower electron density at the ruthenium center, to form an oxometallacycle. An attempt to "force" metallacycle formation was made by starting with the structure in Chart II. Energy minimization of this structure led to a geometry with the C–C bond longer than the strained C–C single bond in ethylene oxide, the terminal carbon bound to one of the nitrogen ligands, and an increased Ru–terminal-carbon distance. These results indicate that oxometallacycle formation is not favored. The formation of a carbon–nitrogen-bonded species is interesting in connection with the so-called suicide complex, a five-membered Ru–O–C–C–N cyclic structure.[12] Optimization of an analogous oxometallacycle with a slightly smaller O–C–C angle than that in **6** led to a bound epoxide minimum.

4. Nonconcerted [1 + 2] Pathways. As for the organic analogue, CH_2: + C_2H_4 → cyclo-C_3H_6. A concerted [1 + 2] addition pathway is unfavorable. Unfavorable orbital interactions, discussed below, lead to nonconcerted (i.e. off-center) pathways. A more detailed analysis of the Ru–oxo/olefin potential energy surface reveals that as far away as ≈2 Å, greater than a covalent C–O bond distance, the perturbation of the ethylene fragment off-center reduces the total energy of the entire system.

Off-center pathways exhibit decreased repulsion between the oxo σ lone pair (largely p_z) and the ethylene π MO (**2a**; see Chart III), increased back-bonding from the oxo σ lone pair to the ethylene π^* MO (**2b**), and increased interaction between the ethylene and Ru–oxo π MO's (**2c**). As shown for **2b** and **2c** in Chart III, the overlaps are zero. Motion in the direction indicated

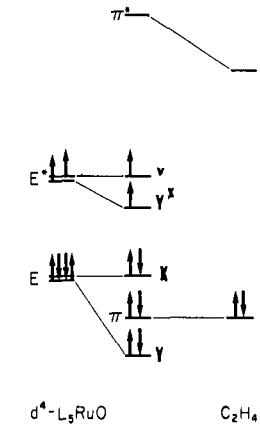

Figure 5. RuL_5O^{2+} + ethylene MO interaction diagram: on-center and perpendicular orientation.

Chart III. Changes in Orbital Interactions Arising from the Perturbation of the Ethylene Fragment to an Off-Center Orientation

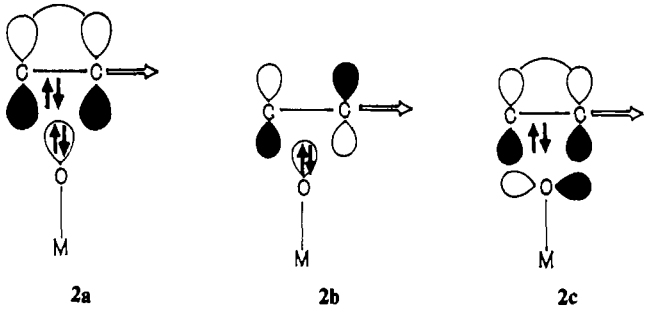

Scheme II. Second-Order Mixing of the Ethylene π and π^* Orbitals Leading to a Polarization of This Orbital

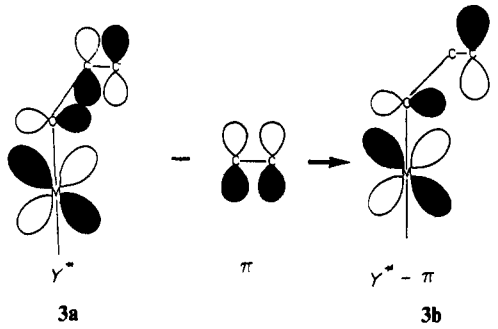

by the arrow will remove this orthogonality and lead to a stabilizing interaction and thus a lower energy pathway. An MO interaction diagram for the interactions between the metal–oxo and olefin π orbitals (on-center and perpendicular orientation) is shown in Figure 5. With this geometry, the ethylene π^* can interact with the Ru–O e and e*, while the ethylene π cannot. Second-order mixing between the π and π^* orbitals is forbidden. Moving the ethylene off-center allows for interaction of the filled ethylene π orbital with the Ru–O Y* (previously the e_y^* part of the no longer degenerate e* pair of MO's), allowing second-order mixing of the C_2H_4 π and π^* MO's. The ethylene π MO is lower in energy than the Ru–O Y* MO and thus adds into it (Figure 5), raising its energy. The net interaction is stabilizing, and the antibonding combination is shown in Scheme II. This is an MO description of a process leading to a species with increased radical cation character on the terminal carbon. This second-order mixing process is very important in two respects. First, it allows for a significant portion of the Y* to be placed on the terminal carbon. Thus, interaction of this orbital with the unperturbed Ru–O X* MO (the unperturbed portion of the e* pair of MO's) can, upon further reaction, lead directly to a bound epoxide minimum. Second, due to the increased electron donation by the ethylene π MO, there is a reduction of electron density on the terminal carbon, which directs the attack of this carbon atom to the

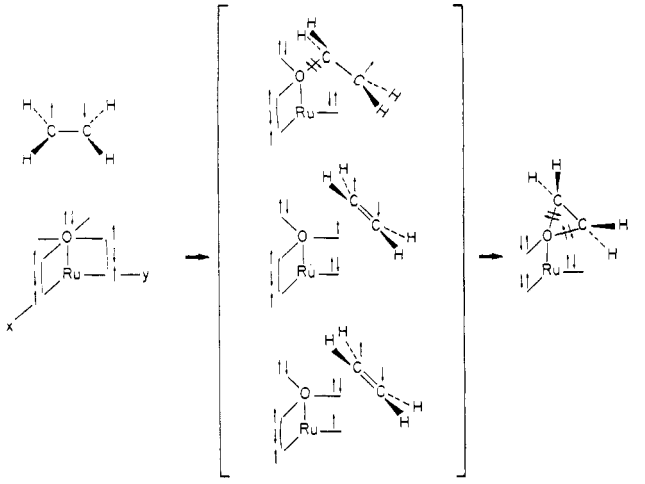

Figure 6. VB interaction diagram of active space for the formation of a bound epoxide.

Chart IV. Diagram Showing the Increased $p\pi-p\pi$ Overlap for Perpendicular (**4a**) vs Canted (**4b**) Ethylene Geometries

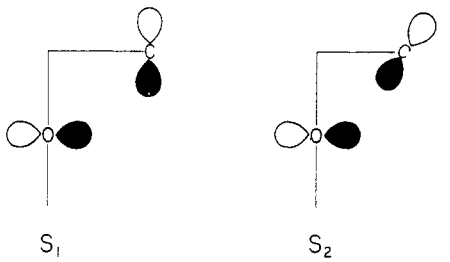

4a **4b**

electron-rich oxygen atom (to yield a bound epoxide minimum) rather than to the electron-poor, high-valent Ru atom (to yield an oxometallacycle).

There is also a clear preference for approach of the ethylene fragment such that its molecular plane is no longer perpendicular to the vector that describes the Ru–O bond. Attack of the C_2H_4 fragment in this way leads to a more stable pathway due to greater overlap between the ethylene and Ru–oxo π symmetry orbitals in the perpendicular (**4a**; see Chart IV) versus canted (**4b**) pathways. Canting leads to a local minimum, bent bound epoxide, which is calculated to be 7.3 kcal mol^{-1} lower than any perpendicular addition mode.

5. Comparison of Proposed Intermediates. Although we cannot quantitatively compare the energy of an optimized stationary point on the PES (i.e. the bound epoxide) with an artificially constructed geometry (i.e. the metallacycle), we should be able to compare these two proposed intermediates to see if the INDO results are supported by qualitative MO reasoning.[28] The oxometallacycle is characterized by σ_{CO} and σ_{MC} bonds and two oxygen lone pairs (derived from the e_x and O p_z). The valence bond diagrams that describe the "motion" of the electrons in the active space for the formation of bound epoxide and oxometallacycle are given in Figures 6 and 7. INDO/1 calculations on oxometallacycle structures point to the M–C σ bond being largely covalent and the M–O σ bond being polarized toward the oxygen. If we assume that the M–C bond is perfectly covalent and the M–O bond ionic, then a d^5, Ru(III) limiting structure results (four electrons in the nonbonding d_{xy} and d_{xz} orbitals, with the fifth being engaged in the M–C bond). The oxometallacycle is, at its most basic level, a seven-coordinate structure, and these have been shown by Hoffmann and co-workers[29] to possess a characteristic frontier orital splitting of two nonbonding d orbitals below three strongly antibonding d orbitals, making a d^5, Ru(III) disfavored. The fifth

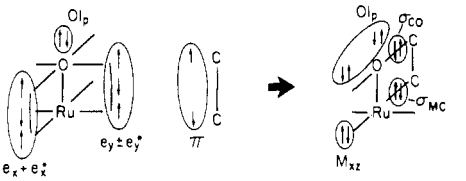

Figure 7. VB interaction diagram of active space for formation of an oxometallacycle.

Ru 4d electron is singlet coupled with an electron in a terminal carbon orbital in an MO that is antibonding between the Ru and C atoms.

The bound epoxide intermediate is a low-spin d^6, six-coordinate structure and thus quite stable. Geometry optimization of a oxometallacycle with the structure shown in Figure 6, as mentioned previously, leads to a bound epoxide. These conclusions, along with the partial charge considerations, point to the favorability of the bound epoxide versus oxometallacycle pathways and intermediates.

6. Comparison of Theoretical Model with Experimental Observation. The theoretical model presented above agrees quite well with experimental observations.[5a] Specifically, the experimental observations are the presence of 5% *trans*-epoxide in the epoxidation of *cis*-epoxide and the slower rate of reaction for *cis*-stilbene. The off-center orientations, which the calculations indicated lead to more stable pathways and local minima, induce a dissymmetry in C–O bonding in the reaction pathway. Geometry optimization reveals that the first C–O bond was essentially entirely formed before the second C–O bond started to form. As the first C–O bond becomes more covalent, the carbon hybridization changes from sp^2 to sp^3, decreasing π bonding and allowing for a reduced C–C rotational barrier. At a point on the potential energy surface, not an intermediate or any other stationary point, prior to the second C–O bond formation, e.g. **5a**, an 8.8 kcal mol^{-1} rotational barrier is calculated. In the epoxidation of *cis*-stilbene at room temperature, 5% isomerized product is found. This is consistent with a somewhat hindered rotation about the C–C bond permitting some rotation before the second C–O bond forms. Recent work[30] on Ru–porphyrin species would seem to indicate that the reverse process, C–O bond breaking and isomerization of the epoxide, may also be feasible. The slower rate for *cis*-stilbene, one order of magnitude less than that for the trans isomer, is consistent with a preference for canted pathways. For the preferred off-center and canted pathway *cis*-stilbene has one sterically hindered trajectory (i.e. both phenyl groups pointing away from the equatorial ligands). Furthermore, experimental and theoretical evidence[31] shows that *trans*-stilbene is planar while *cis*-stilbene deviates markedly from planarity. Thus, for the preferred canted approach modes, the cis isomer is expected to have larger steric repulsions. Comparison with Fe analogues must be tempered by the differences between the Fe–O[23b,32] and Ru–O bonds.[23a,b] There is a larger contribution from ionic configurations in the ground-state wave function for Fe–O in comparison to the Ru–O system.

7. Summary. The successful encounter of the ruthenium–oxo species with the olefin to produce epoxide is envisioned to occur as follows. Concerted [1 + 2] and [2 + 2] cycloaddition pathways suffer from unfavorable orbital interactions that are similar to those observed for their organic analogues; i.e., they lead to repulsions between occupied MO's. As with those for their organic analogues, nonconcerted pathways provide an opportunity to decrease unfavorable interactions and increase favorable interactions. Ethylene attack is directed at the oxo oxygen. Since there is also extra stability to be gained from an off-center approach, a dissymmetry in C–O bonding is induced. A detailed analysis of the oxo/olefin potential surface indicates that these geometric

(28) Zerner, M. C. Personal communication.
(29) Hoffmann, R.; Beier, B. F.; Muetterties, E. L.; Rossi, A. R. *Inorg. Chem.* **1977**, *6*, 55.
(30) Groves, J. T.; Ahn, K. H.; Quinn, R. *J. Am. Chem. Soc.* **1988**, *110*, 4217.
(31) Hohlneicher, G.; Müller, M.; Demmer, M.; Lex, J.; Penn, J. H.; Gan, L.; Loesel, P. D. *J. Am. Chem. Soc.* **1988**, *110*, 4483.
(32) Bagus, P. S.; Preston, H. J. T. *J. Chem. Phys.* **1973**, *59*, 2986.

perturbations occur early on in the interaction. Thus, geometry optimizations indicate that one C–O bond is nearly entirely formed before the second C–O bond begins to form. Since the reaction is a nucleophilic attack by the olefin on the oxo, it is not surprising that a positive charge builds up on the unbound C. In order to take advantage of the greater overlap between the O pπ AO's in the frontier orbital of the Ru–oxo system and the ethylene π system, the olefin cants. This canting motion agrees with the observation that *cis*-stilbene is epoxidized at a slower rate than the trans analogue. Eventually a symmetrically bound epoxide minimum on the potential energy surface is attained, as one would predict from simple electrostatic considerations, with a concomitant two-electron reduction of the metal. The 5% isomerized product formed in the epoxidation of *cis*-stilbene is consistent with the fact that some C–C bond rotation can occur before the formation of the second C–O bond. The relief of steric strain in *cis*-stilbene is obviously sufficient enough to provide a driving force for this rotation. The preference for bound epoxides over oxometallacycles found by INDO/1 is supported by partial charge, frontier MO, and simple electronic structural considerations.

Note Added in Proof. Since the acceptance of this paper for publication, an independent experimental study (Ostovic, D.; Bruice, T. C. *J. Am. Chem. Soc.* **1989**, *111*, 6511) on the related iron–porphyrin systems has presented conclusions similar to those given here.

Acknowledgment. We wish to thank the NSF and the University of Florida for financial support. Helpful discussions with Michael Zerner (University of Florida) and Keith Purcell (Kansas State) are gratefully acknowledged. This paper is based on a lecture presented (by T.R.C.) at the Symposium on Atom Transfer Reactions, 197th National Meeting of the American Chemical Society, Dallas TX, 1989; Paper INOR 267. We wish to thank John Groves (Princeton) for organizing a stimulating symposium and the participants for many profitable discussions.

Contribution from the Department of Chemistry, Faculty of Science, Tohoku University, Aramaki, Aoba-ku, Sendai 980, Japan

Cation Effect on the Quenching of the Photoexcited State of Tetrakis(μ-pyrophosphito-*P*,*P*')diplatinate(II) by Octacyanomolybdate(IV) in Aqueous Solution

Tadashi Yamaguchi and Yoichi Sasaki*

Received November 30, 1988

The photoquenching reaction of $[Pt_2(pop)_4]^{4-}$ (pop^{2-} = pyrophosphite(2–)) with $[Mo(CN)_8]^{4-}$ was studied in 0.01 M HCl or $HClO_4$ in the presence of various added electrolytes (0.49 M) (LiCl, NaCl, KCl, CsCl, NH_4Cl, $(C_2H_5)_4NCl$, and $NaClO_4$) at 25 °C. The quenching rate constants (k_q) differ by nearly 1 order of magnitude from 1.17×10^7 (LiCl) to 9.90×10^7 M^{-1} s^{-1} (CsCl). The phosphorescence lifetime (τ_0) in the absence of the quencher is practically constant (8.3–8.6 μs) regardless of the type of electrolyte added. k_q shows a linear correlation with the reciprocal of the cation Stokes radii except for the case of $(C_2H_5)_4N^+$. The cation effect was interpreted by considering a precursor ion triplet among two negatively charged reactants and a foreign cation. The role of the cation is to reduce the Coulombic barrier of the two reactants in order to form an encounter complex.

In a recent work,[1,2] we showed that the rate of emission quenching of $[(Mo_6Cl_8)Cl_6]^{2-}$ with $[IrCl_6]^{2-}$ in acetonitrile is significantly affected by the nature of added cations (M^+). At $[M^+]$ = 0.1 M, the second-order rate constant (M^{-1} s^{-1}) ranges from 2.7×10^7 for M^+ = *n*-Bu_4N^+ to 1.0×10^9 for Na^+ at 25.0 °C.[1,2] This fact was interpreted by considering that cations assist the encounter complex formation between the two negatively charged reactants. Namely, the ion triplet involving a foreign cation is considered as a precursor to the reaction. A similar drastic cation effect was not observed for the same reaction in aqueous hydrochloric acid media.[2] It is unlikely that the different behavior in the two solvents is directly related to the solvent properties, although water has a much higher dielectric constant and is less favorable for ion-pair or ion-triplet formation. It may be more important that the quenching rate is much faster in aqueous hydrochloric acid and in approaching the diffusion-controlled limit.[2] Significant cation effects have been reported for some thermal electron-transfer reactions in aqueous media.[3-5] A similar cation effect could be observed for a photoquenching reaction in aqueous media, if an appropriate reaction system were chosen.

We have used $[Pt_2(pop)_4]^{4-}$ (pop^{2-} = pyrophosphite(2–))[6,7] as a sensitizer and $[Mo(CN)_8]^{4-}$ as a quencher for the study of the cation effect in aqueous solution. The rate of this quenching reaction is known to be much smaller than the diffusion-controlled limit.[8] With such highly negatively charged reactants, a significant influence of cations is expected on the quenching rate, so far as the reaction proceeds through encounter complex formation and not through a long-distance mechanism.

Experimental Section

Potassium Tetrakis(μ-pyrophosphito-*P*,*P*')diplatinate(II) Dihydrate, $K_4[Pt_2(pop)_4]\cdot 2H_2O$. This compound was prepared by the reported me-

(1) Tanaka, H. K.; Sasaki, Y.; Saito, K. *Sci. Pap. Inst. Phys. Chem. Res. (Jpn.)* **1984**, *78*, 92–96; *Chem. Abstr.* **1985**, *103*, 169703n.
(2) Tanaka, H. K.; Sasaki, Y.; Saito, K. *Inorg. Chem.*, submitted for publication.
(3) Pennington, D. E. In *Coordination Chemistry, Vol. 2*; Martell, A. E., Ed.; ACS Monograph 174; American Chemical Society: Washington, DC, 1978; pp 550–553.
(4) Dennis, C. R.; Leipoldt, J. G.; Basson, S. S.; Van Wyk, A. J. *Inorg. Chem.* **1986**, *25*, 1268–1270 and references cited therein.
(5) Spiccia, L. G.; Swaddle, T. W. *Inorg. Chem.* **1987**, *26*, 2265–2271.
(6) Dos Remedios Pinto, M. A. F.; Sadler, P. J.; Neidle, S.; Sanderson, M. R.; Subbiah, A.; Kuroda, R. *J. Chem. Soc., Chem. Commun.* **1980**, 13–15.
(7) Recent studies on $[Pt_2(pop)_4]^{4-}$: (a) Fetterolf, M.; Friedman, A. E.; Yang, Y.-Y.; Offen, H.; Ford, P. C. *J. Phys. Chem.* **1988**, *92*, 3760–3763. (b) Che, C.-M.; Lee, W.-M.; Cho, K.-C. *J. Am. Chem. Soc.* **1988**, *110*, 5407–5411. (c) Nagle, J. K.; Brennan, B. A. *J. Am. Chem. Soc.* **1988**, *110*, 5931–5932. (d) Che, C.-M.; Kwong, H.-L.; Cho, K.-C. *Inorg. Chem.* **1988**, *27*, 3691–3692. (e) Yamaguchi, T.; Sasaki, Y.; Ikeyama, T.; Azumi, T.; Ito, T. *J. Coord. Chem.* **1988**, *18*, 223–226. (f) Roundhill, D. M.; Shen, Z.-P.; King, C.; Atherton, S. J. *J. Phys. Chem.* **1988**, *92*, 4088–4094. (g) Che, C.-M.; Lee, W.-H.; Cho, K.-C.; Harvey, P. D.; Gray, H. B. *J. Phys. Chem.* **1989**, *93*, 3095–3099. (h) King, C.; Yin, Y.; McPherson, G. L.; Roundhill, D. M. *J. Phys. Chem.* **1989**, *93*, 3451–3455. (i) Roundhill, D. M.; Gray, H. B.; Che, C.-M. *Acc. Chem. Res.* **1989**, *22*, 55–61 and references cited therein.
(8) Ueno, F. B. Ph.D. Thesis, Tohoku University, 1982.

0020-1669/90/1329-0493$02.50/0